Remote Sensing Applications: Society and Environment 39 (2025) 101710

Contents lists available at ScienceDirect

Remote Sensing Applications: Society and Environment

journal homepage: www.elsevier.com/locate/rsase

A novel random forest approach to downscale SMAP soil moisture products to 100 m resolution using temporally closest satellite observation data

Mohsen Moghaddas *, Massoud Tajrishy

Department of Civil Engineering, Sharif University of Technology, Azadi ave., Tehran, Iran

ARTICLE INFO

Keywords:
Downscaling soil moisture
Multi-satellite data integration
Google earth engine (GEE)
REMEDHUS soil moisture network
Random forest modeling

ABSTRACT

Surface soil moisture is an important factor in controlling the water and energy budget, as well as other hydrological and land surface processes. However, the coarse resolution of satellite data monitoring soil moisture presents a problem that can be addressed by downscaling. This study presents a novel approach for downscaling the coarse-resolution Soil Moisture Active Passive (SMAP) soil moisture product using a random forest model with data from Landsat, MODIS, Sentinel-1, and Sentinel-2 satellites. Key variables include vegetation indices, land surface temperature (LST), low-resolution microwave data, and elevation. Leveraging Google Earth Engine (GEE), individual models are developed for each SMAP image, using the closest finer satellite data to account for temporal variations and enhance prediction accuracy. The downscaled product was evaluated across various spatiotemporal scales and land cover types, showing strong correlations with precipitation and irrigation events, high efficacy in water body detection, and differentiation between crop types and moisture conditions. Comparisons with soil moisture time series from Spain's REMEDHUS network indicate good agreement, with an R-value of 0.697 and an RMSE of 0.098 m^3/m^3, very close to its much coarser resolution counterpart SMAP/Sentinel-1 1 km product with RMSE 0.07 m^3/m^3, highlighting the downscaled product's robustness and accuracy. Developing the model for each target soil moisture product, as opposed to a single model for all images, reduces the time and volume of the training phase while maintaining prediction accuracy. This study's findings suggest that downscaling soil moisture data to 100 m resolution significantly enhances the ability to monitor and manage soil moisture at a finer scale. This improvement has broad implications for precision agriculture, hydrological modeling, and environmental monitoring, potentially leading to better resource management, improved crop yields, and more accurate hydrological predictions.

1. Introduction

Surface Soil Moisture (SSM) is a key variable in controlling the water and energy budget of the land ecosystem (Brocca et al., 2010; Petropoulos et al., 2015). It is crucial in driving hydrological and land surface processes (Ochsner et al., 2013). Accordingly, SSM estimation and the knowledge of its dynamic is valuable in many applications such as drought(Martínez-Fernández et al., 2016; Sánchez et al., 2018) and flood monitoring (Abushandi, 2016; Kim et al., 2018),evapotranspiration estimations (Martens et al., 2016;

* Corresponding author.
E-mail address: mohsen.moghaddas96@gmail.com (M. Moghaddas).

https://doi.org/10.1016/j.rsase.2025.101710
Received 8 November 2024; Received in revised form 6 June 2025; Accepted 29 August 2025
Available online 2 September 2025

Purdy et al., 2018) and water resources management (Kerr et al., 2010; Koster et al., 2018). In addition, recent advancements in high-resolution soil moisture observation enable new applications such as routine slope condition updates for landslide prediction and improved flash flood forecasting, both of which demand spatially dense and temporally relevant data (Brocca et al., 2023).

Remote sensing methods can provide a practical means for estimating soil moisture at regional and global scales when no prior data is available (Brocca et al., 2012). Microwave (MW) remote sensing can detect surface SM content directly by utilizing the dielectric difference between dry soil and liquid water. Because passive microwaves are less affected by vegetation, soil surface roughness, topography, and water content, they can provide more accurate surface SM estimates (Entekhabi et al., 2010; Piles et al., 2014). Among all MW frequencies, L-band (1–2 GHz) can penetrate through the atmosphere and moderate vegetation and is optimal for soil moisture measurements (Kerr et al., 2010).

Soil Moisture Active Passive (SMAP) (Entekhabi et al., 2010) and Soil Moisture and Ocean Salinity (SMOS) (Kerr et al., 2010) are two L-band passive MW missions providing SM globally every 1–3 days (Ma et al., 2019), However, coarse-resolution passive microwave SM data (>10 km) cannot provide detailed surface SM distributions needed for many hydrological and agricultural applications. Therefore, fine-resolution auxiliary data from other satellite or in-situ measurements have been used to downscale the coarse-resolution data based on surface SM distributions. These approaches leverage the higher temporal granularity of passive MW measurements from SMAP and SMOS and combine them with higher resolution but less frequent thermal and optical imagery through downscaling approaches to create a soil moisture product with higher spatial and temporal resolution.

For a thorough examination of the current SM downscaling algorithms and the ancillary inputs they necessitate, refer to (Peng et al., 2017). Additionally, for a review of various techniques along with the advantages and disadvantages of different downscaling approaches, see (Sabaghy et al., 2018). The ML-based techniques seem better options for downscaling due to 1. not requiring concurrent overpasses by other satellites and 2. data is not required in a continuous manner which enables us to use satellite data in a larger period. Many researchers have tried to reduce the resolution of remotely sensed data using different machine learning methods, in one of the first studies in this scope (Chai et al., 2011) an artificial neural network (ANN) model based on Moderate Resolution Imaging Spectroradiometer (MODIS) data used for downscaling Polarimetric L-band Multibeam Radiometer (PLMR) L-band data from 20 Km resolution to 1 Km which reached the accuracy of RMSE = 0.018–0.035 $m^3\ m^{-3}$, this result demonstrates a highly promising level of accuracy for this class of downscaling methods.

Several studies compare the performance of random forest models using different auxiliary data, one of this research (Bai et al., 2019), trained five random forest (RF) models under different auxiliary data driven by MODIS and Sentinel-1 (LST, leaf area index (LAI), and normalized difference vegetation index (NDVI) from MODIS, VV polarization from Sentinel-1 and digital elevation model (DEM)) and compared the performance between them. Also another study (Zhao et al., 2018) used four data combinations of MODIS (AM + Terra, PM + Terra, AM + Aqua, PM + Aqua) to train different RF models for downscaling SMAP and SMOS, results indicated similar good performance for all combinations, with an unbiased root-mean-square difference of 0.022 m^3/m^3. Several other researchers (Jin et al., 2021) integrate two or more machine learning models for downscaling coarse-resolution data.

The above studies and more investigations (Chen et al., 2020; Sishah et al., 2023) nominate random forest models are better for downscaling soil moisture data using high-resolution remote sensing data (Table 1 presents some selected studies), the reason is that the random forest model is more flexible with randomization that coincides with the nature of soil moisture. The model trains using

Table 1
Review of selected random forest studies for downscaling SMAP soil moisture data.

study	Spatial resolution	Model training	Auxiliary data	Final resolution	validation
Gao et al. (2024)	9 KM	data collected from May to September 2021, which is the non-freezing period of the soil	the normalized difference soil index (NDSI) and bare soil index (BSI), LST, NDVI, elevation, Albedo	1 KM	19 % Enhanced the model accuracy by using the Soil indexes (NDSI and BSI) as auxiliary data at the Weigan river basin
Sishah et al. (2023)	36 KM	An RF model trained with one year of data	Vegetation Indexes and LST from MODIS, Soil grids (texture, density, and organic carbon), CHIRPS, modified SAR data	1 KM	20 soil samples in the wet and dry seasons (Awash River basin), with 0.53 correlation value
(Nadeem et al., 2023)	9&36 KM	An RF and ANN model trained over the 2018 year	MODIS VI's indexes and rainfall data	1 KM	Stations over the ShanDian river basin with ubRMSE 0.034 m^3/m^3
(Wakigari and Leconte, 2022)	9&36 KM	RF model with summer season's data from 2017 to 2020	NDVI, Albedo and LST from MODIS, Sentinel-1 (VV and VH), DEM (slop and aspect)	1 KM	SCAN and USCRN network with R-value of 0.86 for 36 km and 0.91 for 9 km
(Sun et al., 2020)	36 KM	DSCALE_mod16(a mathematical model)	MODIS ET's data, gridded meteorological data	500 m	At three different sites with ubRMSEs from 0.026 to 0.055 m^3/m^3
Chen et al. (2020)	36 KM	Trained an RF model over the 2019 year	VI's and LST from MODIS, DEM (slop and aspects), LST	1 KM	Compared with 6 km CDAS (RMSE = 0.03 m^3/m^3) and 25 km GLDAS (RMSE = 0.08 m^3/m^3)
(Bai et al., 2019, p. 2)	9 KM	Five RF models over one year (August 2017 to 2018) with different combinations of auxiliary data	VI's and LST from MODIS, VV of Sentinel-1, DEM (slop and aspect)	3&1 KM	At four stations during this year with ubRMSE from 0.033 to 0.023 cm^3/cm^3

vegetation indexes (NDVI, Soil Adjusted Vegetation Index (SAVI), enhanced vegetation index (EVI), and …) as well as other surface characteristics. The input variables were Synthetic Aperture Radar (SAR) data, optical data, and topography data, and the final output variable was SSM. As shown in Table 1, previous studies have utilized datasets spanning one year or more to train a single random forest model for the downscaling of various SMAP products.

Today, cloud computing platforms equipped with supercomputers provide the opportunity to develop models more rapidly without the necessity of downloading large volumes of data(Chi et al., 2016). Google Earth Engine enables the creation of distinct models for each target product. Specifically, we utilize different datasets to train a unique model using the nearest auxiliary data corresponding to each SMAP image. This approach offers three primary advantages compared to previous studies. First, the model is developed with a smaller volume of auxiliary data, which significantly reduces training costs. Second, the selection of data can be tailored to the conditions of the target image. For instance, we can choose the time span of the training data based on the soil moisture memory relevant to our study area. Third, we circumvent issues related to model transferability, allowing this approach to be implemented in any study area seamlessly.

Two separate models were developed for each image; Initially, based on MODIS indexes (NDVI, EVI, LAI, LST, normalized difference water index (NDWI), Land Cover), topography data, and SAR data to downscale 10 km SM product to one KM data. Subsequently, using NDVI, NDWI, EVI, and Normalized Difference Moisture Index (NDMI) indexes from Sentinel-2, SAVI, and EVI from Landsat8 with topography data, and SAR data to downscale 1 km product to 100 m products. Output results are evaluated and validated with two criteria, 1) precipitation time series in Iran and 2) REMEDHUS stations in Spain.

The paper is organized as follows: In the next section, case studies, as well as datasets and satellite data that are used for modeling and validation, are represented, then in section three, an overview of the downscaling technique is presented, likewise a representation of the soil moisture results is provided in section four, and in the two final sections, we evaluate the results for validation and discussion about outputs.

2. Data and study area

In the following section, we describe the datasets used in this study, i.e. in-situ data of ISMN network, precipitation data, Sentinel-1 backscatter, Landsat-8 (L8), Sentinel-2 optical data, and MODIS data. Our analysis focuses on the year 2020 and Google Earth Engine

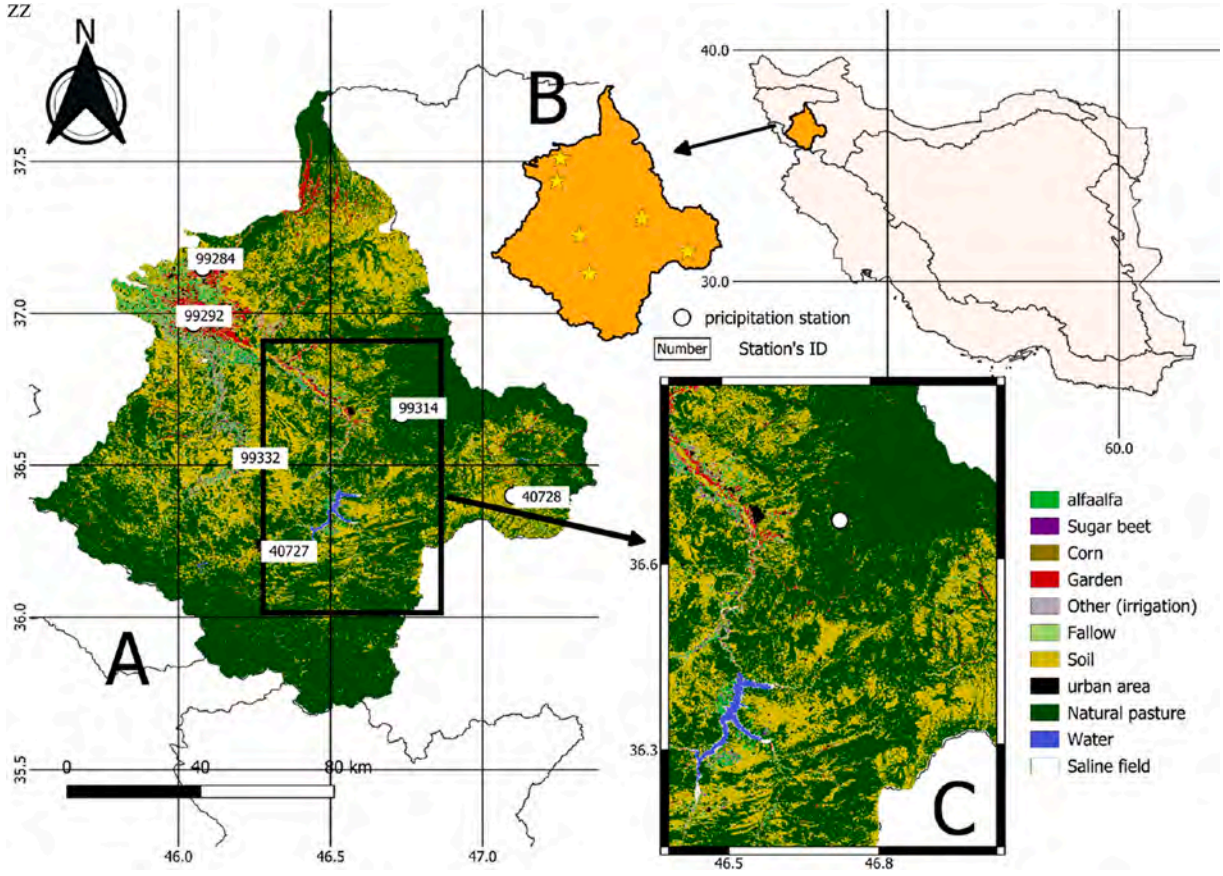

Fig. 1. Simineh-Zarineh river basin location in Iran, elevation map, and Landsat visualization.

(GEE) made available all data except ISMN and precipitation data. The training set included nearly 2000 samples.

2.1. Study areas

Two study areas were investigated in this research.

2.1.1. Simineh-Zarineh river basin

Simineh-Zarineh river basin is located in the south and southwest of Urmia Lake in Iran. From the view of extent, it is the first sub-basin of the Urmia Lake Basin. Its coordinates in the east-west direction are from 45°27′38.2″ to 47°21′56.3″ and in the south-north direction are from 35°40‘8.3″ to 37°44′13.1’’. The elevation range in this area from 1260 m to 3380 m is variable. The average annual temperature in this region is 11.2 °C and the average annual precipitation and evaporation are 341 and 1200 mm/year, respectively(Djamali et al., 2008).

2.1.2. Duero river basin (REMEDHUS network)

A basin in the center of Spain is an area also chosen for downscaling in the present study. The majority of the land in this region is croplands and shrublands, and it is located about 650 m above sea level. There is a semiarid Mediterranean climate in the region, which is characterized by hot, dry summers and cold, mild winters (Ceballos et al., 2005). Fig. 2 shows the REMEDHUS soil moisture observation network in the center of the study area. The network is located in a flat area of about 1225 square km (41.1–41.5° N, 5.1–5.7° W), with elevations between 700 m a.s.l. and 900 m a.s.l. Precipitation and temperature average 385 mm and 12 °C, in order. The land use of the network Is divided into rainfed cereals (78 %), forest and pasture (13 %), irrigated crops (5 %), and vineyards (3 %) (Sánchez et al., 2012). At the soil moisture stations, capacitance probes are used to measure soil moisture at hourly intervals in the top layer (5 cm).

2.2. Data

2.2.1. Ground-based data

The ISMN was established as a global in-situ soil moisture database, its website accessed on February 28, 2020 (https://ismn.geo.tuwien.ac.at), through which data from hundreds of worldwide stations are available. We used the REMEDHUS network in Spain which is provided by Universidad de Salamanca with 19 active stations. Daily records of precipitation were taken from six synoptic stations of the Iran Meteorological Organization (IMO) from the year 2020 for time series validation of soil moisture (Fig. 1). These

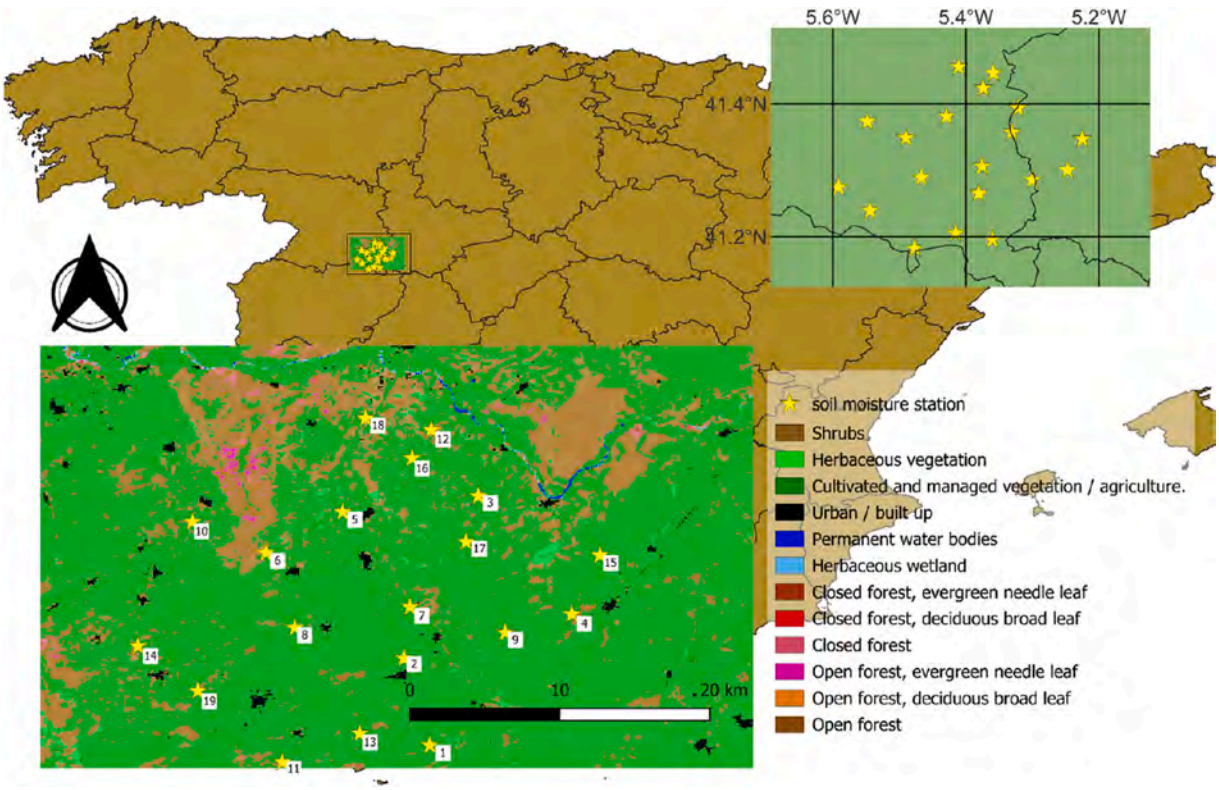

Fig. 2. Location of REMEDHUS network stations on the elevation map of 2.2.2. SMAP Soil Moisture.

stations are located inside Simineh-Zarineh river basin in Iran.

The SMAP satellite was launched on January 31, 2015 with L-band missions aimed at generating soil moisture products over the globe. The SMAP orbit is a near-pole with overpass ascend and descend times at 6:00 p.m. and 6:00 a.m. local time. The satellite mission was to produce a soil moisture map with three resolutions: 36 km passive (O'Neill, Peggy E. et al., 2018, p. 3), 9 km active-passive (Entekhabi et al., 2010), and 3 km active radar. However, a failure occurred in the radar on July 7, 2015 that caused limitations in active and active-passive product generation. Nevertheless, SMAP passive soil moisture products have an important role in recording and monitoring soil moisture with an accuracy that meets all mission requirements (Chen et al., 2018). In this study, NASA-USDA Enhanced SMAP Global Soil Moisture Data was used. This product is a 3-day composite product generated by NASA GSFC, containing global estimates of SSM including ascending and descending half-orbit estimates. It is available from April 1, 2015 until August 2, 2022 (https://gimms.gsfc.nasa.gov/SMOS/SMAP/) for the whole world. We downscaled SSM data from the year 2020.

2.2.2. MODIS products

SSM and the other surface variables must be related in any downscaling scheme. As demonstrated by previous downscaling studies, LST, NDVI, EVI, surface albedo, LAI, and NDWI are extremely useful in expressing the relationship between them and SSM (Chauhan et al., 2003; Peng et al., 2015; Sánchez-Ruiz et al., 2014; Zhao and Li, 2013). As a result, each of these variables was obtained from the corresponding MODIS products, including Terra Vegetation Indices (NDVI and EVI) 16-Day Global 250m (MOD13Q1), Terra Leaf Area Index/FPAR 8-Day Global 500m (MOD15A2H), Terra Land Surface Temperature and Emissivity Daily Global 1 km (MOD11A1.061) and MODIS Terra Daily NDWI (available from 2020). For the LST product, the sensitivity analysis conducted in a previous study (Peng et al., 2015) emphasized the importance of daytime LST as an expression of SSM. Additionally, another study (Pablos et al., 2016) found that downscaling results using MODIS daytime LST performed better than those using MODIS nighttime LST.

2.2.3. Landsat8 products

Landsat 8 is a satellite governed by the USGS, providing Earth imagery with a spatial resolution from 30m to 100m every 16 days. Two instruments acquire data from this Satellite, the Operational Land Imager (OLI) and the Thermal Infrared Sensor (TIRS). Data in the GEE data collection USGS L8 Surface Reflectance Tier 1, which consists of atmospherically corrected surface reflectance for red visible and near-infrared (NIR) bands, have been regarded as features for surface vegetation indicators (Chander et al., 2009). Landsat SAVI and LAI were extracted from these satellite images.

2.2.4. Sentinel-1 and Sentinel-2

Sentinel-1 is a C-Band SAR labored inside the Copernicus program, a joint invention of the European Fee (EC) and the European Space Agency (ESA). The usual acquisition mode is the Interferometric Wide Swath Mode (IW), with acquisitions at a 250 km huge swath and a spatial resolution of five in 20m. S1 rotates in a near-polar, solar-synchronous orbit with a 12-day repeat cycle. The two satellites A and B percentage the same orbit plane with a 180° orbital phasing distinction, which leads to a 6-day repeat cycle for the S1 constellation. The information available on GEE provides dual-polarization (VV + VH) ground range Detected (GRD) product (Fletcher & European Space Agency, 2012) which we used VV polarization due to more sensitivity on soil moisture than VH (El Hajj et al., 2017).

ESA expanded the Sentinel-2 mission as part of the EU Copernicus program, with two satellites orbiting together (Sentinel-2A and Sentinel-2B) in 2017. Both incorporate an optical sensor (Multi-Spectral Instrument) the same as those in the Landsat satellites, though they have higher spatial, temporal, and spectral resolutions. MSI covers the globe at 10 or 20m, depending on the spectral band, with a revisit time of 10 days (since June 2015, when Sentinel-2 A was launched) and 5 days (since March 2017, when Sentinel-2B was launched). As a result of the overlap between adjacent orbits, 2–3 days of revisit time can be obtained in mid-latitudes by combining both satellites (Gascon et al., 2017). we used Sentinel-2 MSI Multispectral Instrument Level-2A (L2A) to extract NDVI, NDWI, EVI and NDMI.

2.2.5. Elevation

The NASA Shuttle Radar Topography Mission (SRTM) DEM, version 2.1, obtained from the land processes distributed archive center (https://lpdaac.usgs.gov/), supplied the topographic factors (elevation and slope) for the downscaling study in addition to the above satellite data.

3. Methodology

Machine learning techniques such as random forest (Breiman, 2001) are widely used for classifying, regression, and prediction. To reduce over-fitting, RF uses multiple weak classifiers (decision trees) in an ensemble learning model, in other words, after generating a large number of trees, they pick up the most popular class. We call these procedures random forests. Accordingly, the RF model outputs are the mean predicted values of all independent decision trees in a regression model. RF is suitable for complex and highly nonlinear relationship models due to its adaptive, randomized, and decorrelated features. In comparison to other models, RF is simple, flexible, and less affected by hyperparameters (hyperparameters are the tuning controls that adjust how a machine learning model learns from data) compared to others. It has also been shown in previous studies that the RF model is effective in complex nonlinear fitting and that it can be used to downscale SM models (Im et al., 2016; Zhao et al., 2018). The 9 km SMAP enhanced (Chen et al., 2018), and the 1 km SMAP/Sentinel-1 soil moisture data (Das et al., 2019) products have been shown to contain significantly more detail compared to the original 36 km SMAP product (Lawston et al., 2017; Zhang et al., 2019; Jalilvand et al., 2021). However, many complex factors still affect soil moisture distribution at finer scales, including topography, vegetation, surface temperature, and soil hydraulic properties,

which cannot be fully captured at coarser resolutions (Peng et al., 2017). Meanwhile, RF is known for its low out-of-bag error (good generalization capability) and robustness against overfitting (Breiman, 2001; Belgiu and Drăguţ, 2016; Breiman, 2001)To downscale SMAP SM products, fine-resolution auxiliary data are utilized to obtain detailed information. The general process of downscaling SMAP SM (in two separate stages) is shown in Fig. 3. Surface soil moisture data from SMAP at 10 Km resolution is the target variable also auxiliary data is represented in Fig. 3 also mentioned in Table 2.

There are some considerations for the auxiliary data described in Table 2. First, C-band radar penetrates the soil surface to measure soil moisture directly. VV (Vertical Transmit-Vertical Receive) polarization is more related to soil moisture changing and less influenced by vegetation and soil surface roughness in comparison with VH (Vertical Transmit-Horizontal Receive) polarization (El Hajj

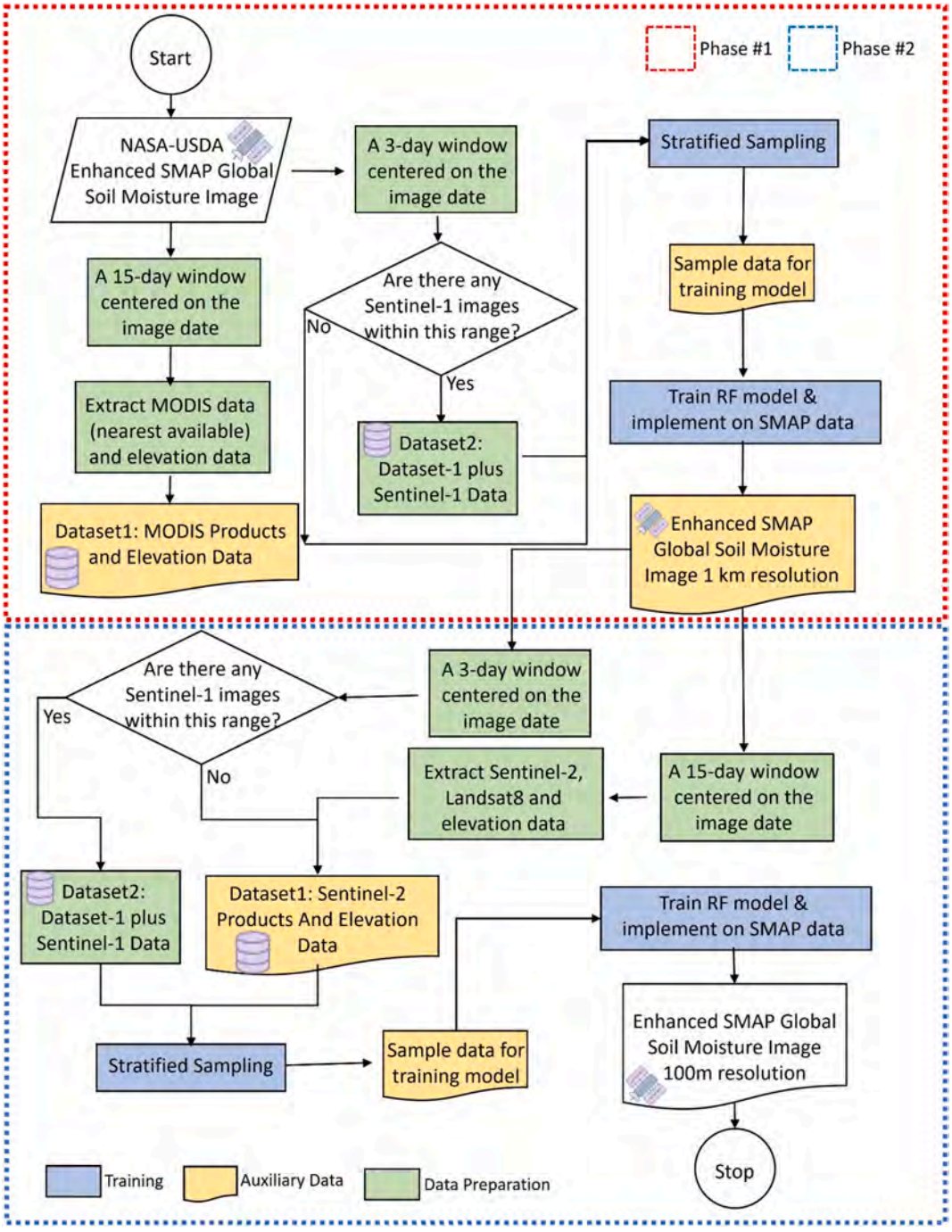

Fig. 3. Downscaling flowchart.

et al., 2017). Furthermore, the share to and debilitation of vegetation on the total backscattering coefficients from Sentinel-1 SAR data can be described with vegetative indexes from optical data (El Hajj et al., 2017). Also, for reducing the surface roughness error we involve LST. Second, selecting the feature space of vegetation indexes (like NDVI, EVI, NDWI, and LAI) and LST is an axial physical foundation for downscaling SM (Choi and Hur, 2012). Third, considering the influence of topographical changes on the earth's surface on the surface energy and surface backscatter, the slope and elevation parameters were selected as input variables as criteria to express this effect (Han et al., 2018). Fourth, according to soil moisture memory that depends on soil properties and other meteorological and biophysical variables of soil, we employed only S1 data recorded a maximum of three days (Lower or greater depending on specific information about the case study area) apart from the moisture date due to the geographical characteristics of the studied area (Martínez-Fernández et al., 2021).

Nevertheless, it is also important to outline the weaknesses of the RF models in this study. First, microwave penetration in soil depends on SM content, soil texture, and microwave frequency (Owe and Van de Griend, 1998). SMAP works in the L-band (penetration about 5 cm in soil) and Sentinel-1 works in the C-band (penetration about 2 cm in soil) so the depths of penetration are different. However, using Sentinel-1 SAR data to downscale coarse-resolution SMAP SM may be beneficial (He et al., 2018; Santi et al., 2018). Second, a significant difference could exist between MODIS daily LST values and those values that exist during SMAP acquisition (Piles et al., 2011). Additionally, an SMAP L-band satellite can measure a depth of 5 cm over bare soils, whereas a MODIS sensor of thermal infrared can measure a depth of 1 mm and the two depths' thermal regimes may be quite different (Entekhabi et al., 2010; Piles et al., 2011). Nonetheless, using LST data to downscale coarse-resolution SMAP SM may be beneficial (Amazirh et al., 2019; El Hajj et al., 2017; Im et al., 2016; Piles et al., 2011).

Therefore, two RF models are established for two stages of downscaling (equations(1) and (2) show the RF models formula.)

$$SM_1 = RF\left[NDVI.\ EVI.\ LAI.\ LST.\ NDWI.\ Elevation.\ Slop.\ Land\ cover.\ \sigma^0_{vv}(if\ exist)\right] \quad (1)$$

and

$$SM_2 = RF\left[NDVI.\ NDWI.\ EVI.\ NDMI.\ SAVI.LAI.\ Slop.Elevation.\ \sigma^0_{vv}(if\ exist)\right] \quad (2)$$

The process of downscaling involves the following steps.

1. Select an SMAP global soil moisture product on a specific date.
2. Select the nearest available auxiliary products by date. (at max 8 days difference, due to the 16 days-once product like NDVI, EVI, and …)
3. If there is S1 data three days (the duration should vary based on the soil moisture memory in the case study) apart from the target date use that, or else, don't use S1 data as an input for the model.
4. Take a 100-point sample of each auxiliary product for training the RF model with a stratified random sampling method (Cochran, 1946) (which is suitable for populations that can be partitioned into sub-populations).
5. Train the RF model with sample data relative to soil moisture target value.
6. Apply the trained RF model over the coarse-resolution SMAP products to extract fine-resolution downscaled data.

4. Results

4.1. Parameter importance

Based on the range and distribution of 10 Km samples, the importance of the different variables was analyzed using the Mean Decrease in Accuracy (MDA) method, as implemented in the Google Decision Forests framework. This method estimates how much the model's predictive performance decreases when the values of a given variable are randomly permuted, thereby indicating the relative

Table 2
Input data (features) used for downscaling SMAP products.

Product	Satellite	Spatial and temporal resolution	Source
NDVI	MODIS	250 m–16 days	MOD13Q1.061 Terra Normalized Difference Vegetation Index
NDVI	Sentinel-2	10 m–10–12 days	Harmonized Sentinel-2 MSI: Multispectral Instrument, Level-2A
EVI	MODIS	250 m–16 days	MOD13Q1.061 Terra Enhanced Vegetation Index
EVI	Sentinel-2	10 m–10–12 days	Harmonized Sentinel-2 MSI: Multispectral Instrument, Level-2A
LAI	MODIS	500 m–8 days	MOD15A2H.061: Terra Leaf Area Index
LAI	Landsat8	30 m – 8days	USGS Landsat 8 Level 2, Collection 2, Tier 1
LST	MODIS	1 Km – daily	MOD11A1.061 Terra Land Surface Temperature and Emissivity
NDWI	MODIS	500 m–16 days	Terra Daily Normalized Difference Water Index
NDWI	Sentinel-2	10 m–10–12 days	Harmonized Sentinel-2 MSI: Multispectral Instrument, Level-2A
VV product	Sentinel-1	10 m–12 days	Sentinel-1 SAR GRD VV polarization
NDMI	Sentinel-2	10 m–10–12 days	Harmonized Sentinel-2 MSI: Multispectral Instrument, Level-2A
SAVI	Landsat8	30 m – 8days	USGS Landsat 8 Level 2, Collection 2, Tier 1
DEM/Slope	GTOPO30	1 Km – Yearly	GTOPO30: Global 30 Arc-Second Elevation
DEM/Slope	SRTM	30 m - Yearly	NASA SRTM Digital Elevation

contribution of each variable to the model's accuracy (Fig. 4). As we can see, the most important variable in both stages is elevation extracted from DEM, stage one of downscaling LST and NDVI have the most impact on model output, also in stage two LAI and SAVI are the important ones. As the literature discussed (Peng et al., 2017) the importance of topographical features is more than other parameters when the downscaling scale gets finer, also the finer the resolution, the more important the topographical feature become (in Fig. 4 the importance of DEM increased compared to other variables at step two of downscaling from 34.8 % to 40.5 %). Further, land cover patterns should have the least importance in downscaling finer products (it is satisfied in stage one so we do not conduct this type of data for the next stage). Moreover, Fig. 4 reveals that the importance variables hover around 10 % across both stages of downscaling. This consistency suggests that all variables exert a significant influence on the output, thereby validating the decision to incorporate a comprehensive set of variables in our model development process. In essence, the inclusion of additional data contributes positively to the creation of robust downscaling models. This assertion aligns with the inherent mechanism of random forest models, which leverage input variables to identify the most influential predictors. By enriching the dataset with more relevant variables, we inherently enhance the model's capacity to capture the nuances of the target variable, thereby improving its overall performance. Furthermore, in our methodology, we omitted the utilization of Sentinel-1 images for downscaling instances where the temporal gap between SMAP and Sentinel-1 exceeded three days. Our analysis reveals that the importance attributed to these data stands at approximately 7 %. This finding suggests that our decision to exclude Sentinel-1 images in such scenarios does not significantly compromise the downscaling process.

4.2. Comparing downscaled 100m and the baseline 10 Km SMAP soil moisture data

In Fig. 1-A land cover map of the Simineh-Zarineh river basin was represented at 10-m resolution (produced by FAO). For a better display soil moisture map, an area of the basin (Fig. 1-C) is selected which contains all class types. The representation of the downscaled product in comparison with an original map for three selected months (May, August and November) is shown in Fig. 5. The water area in the red rectangles is separated from the land features. Additionally, we have made the basin network in the middle and mountain areas on the right side of the map bold and well-defined in the downscaled version.

4.3. Validation against in-situ data

In this section, the validity of the downscaled product responds to the available in-situ and station data in different aspects such as temporal behavior and proximity to the ground data.

Fig. 6 shows the time series of SMAP surface soil moisture data, downscaled SMAP data, and daily precipitation of synoptic stations which are presented in Fig. 1. SMAP SSM data and downscaled SSM data showed good temporal consistency, despite their large-scale differences, it appears that the downscaled SSM preserves the feature of temporal changing of the SMAP SSM in a significant manner. Moreover, the downscaled product has stronger ups and downs in the rainy periods (specifically end of November and between March and May) related to better recognition of soil moisture responding to evaporation or infiltration. In addition, despite the coarse resolution of SMAP products that have a constant trend in periods without precipitation, the downscaled time series show a fluctuation trend in periods without precipitation (Precipitation-free periods in July and September) which corresponds to human activities.

SM time series for the REMEDHUS network (Fig. 2) was calculated and compared pixel-to-point with in-situ data. REMEDHUS

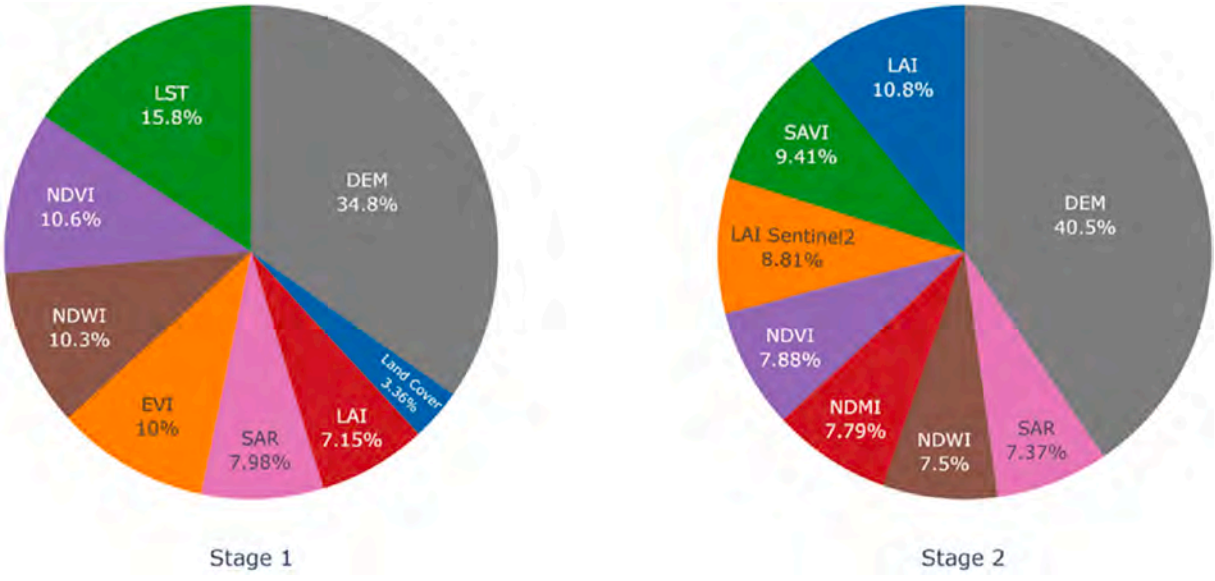

Fig. 4. (a) the variable's importance in stage one of downscaling (b) the variable's importance in stage two of downscaling.

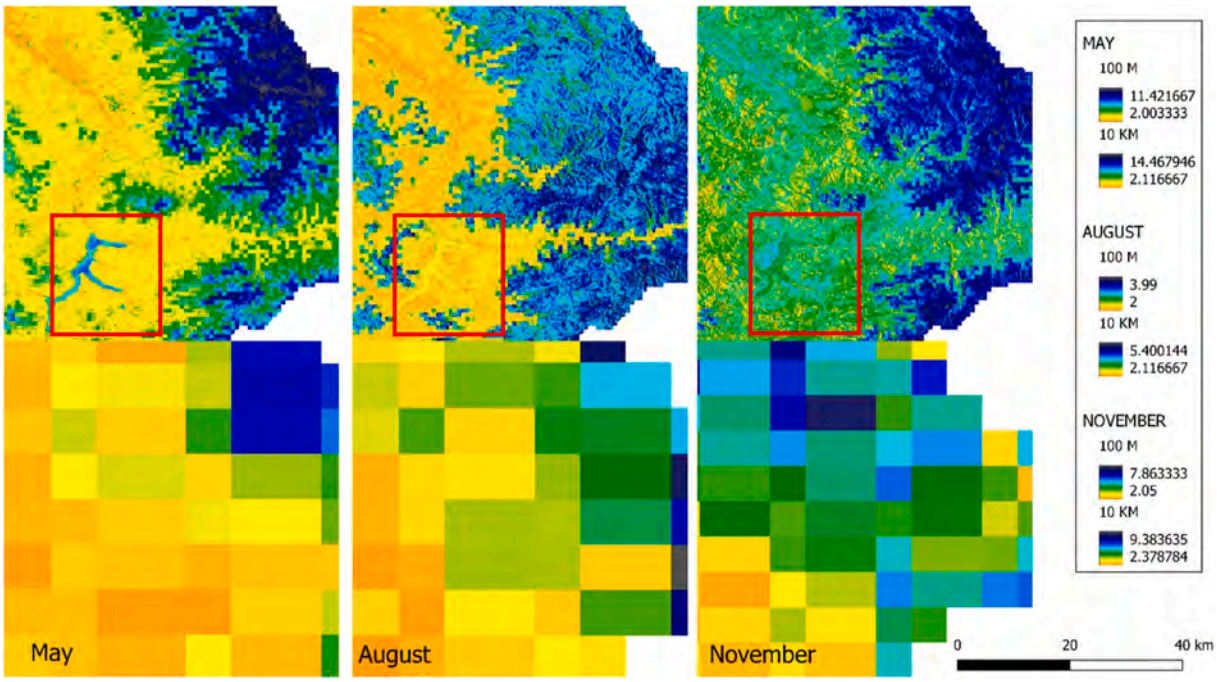

Fig. 5. Three months (May, August, and November) downscaled and original SMAP products.

network record SSM every hour, we select data from the overpass time of SMAP and compare them with downscaled values. The time series of the downscaled product and in-situ data show a precise time concordance in the changes (Figs. 7–10- Left).

The normalized value of satellite SM concerning in-situ measurement is represented in Figs. 7–10. The average R2 score in all stations is 0.697 suggesting a strong positive relationship (this means that the model explains about 70 % of the variance in the observed data) with an RMSE value of 0.098 m3/m3. As discussed, the model tends to underpredict soil moisture values in the majority of cases.

5. Discussion

5.1. Model architecture and auxiliary data

In the development of the model, we exclusively utilized the temporally nearest auxiliary satellite data to construct a specialized model for each SMAP image. This approach enhanced our ability to control the downscaling process and eliminated irrelevant or erroneous data within the study area. For instance, as demonstrated by recent studies (Mao et al., 2022), accounting for soil moisture memory in the selection of auxiliary data is crucial for enhancing model accuracy. Previous studies have employed Sentinel-1 data to train models without considering the temporal interval with SMAP images, resulting in errors in the final output. This oversight can lead to inaccuracies, as surface soil moisture conditions can fluctuate significantly over short periods due to various factors such as heatwaves (McColl et al., 2019) or even influence of growing seasons (De Queiroz et al., 2020).

Typically, all random forest models for downscaling soil moisture products are trained with auxiliary data such as soil texture, topography, vegetation indices, or optical and thermal infrared observations (as detailed in the introduction and methodology sections). However, previous studies have often used a limited variety of such data. For example, they might only use MODIS vegetation indices or a combination of vegetation and topographical indices due to the extensive training sets required when utilizing a year or more of data. The large volume of training data in these studies has restricted the variety of data they could employ. In contrast, by focusing on the quantity of data, our study enables the use of a wider variety of data, which provides a better approach for training a random forest model to downscale soil moisture products.

Since the model relies on the original 10 Km soil moisture data as a reference for prediction, the accuracy of this dataset inherently influences the precision of the 100m output. In instances such as the May output (Figs. 5 and 11), where all auxiliary data are available, the model effectively assigns higher soil moisture values to water bodies. However, a notable bias in the model constrains soil moisture values within the range of the original image. As a result, while the model may assign high soil moisture values to water bodies, it typically refrains from attributing maximum soil moisture values to such areas due to this inherent limitation.

To address this limitation, integrating in-situ soil moisture data into the model development process could be beneficial. By incorporating ground-truth measurements, the model gains access to more accurate and localized soil moisture information, improving its ability to differentiate between land and water surfaces. This approach could mitigate the bias stemming from the reliance on the

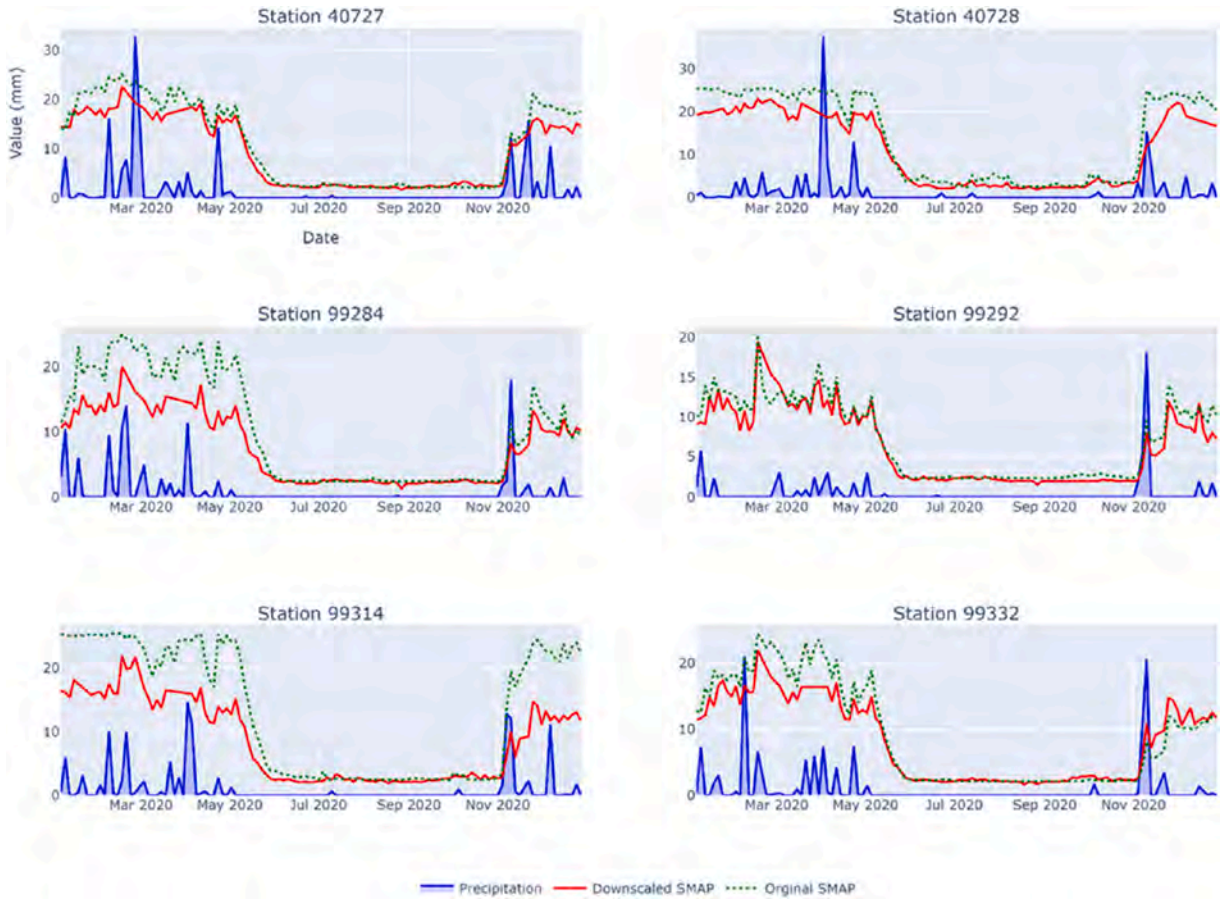

Fig. 6. Time series of original SMAP products and downscaled SMAP in comparison with precipitation.

original 10 km soil moisture data and enhance the model's performance in accurately predicting soil moisture values, particularly in areas with distinct land-water boundaries (Fig. 11).

Additionally, because the model is trained separately for each image, it effectively maintains spatial continuity even when pixel values lack geographic consistency. This capability is evident in cases like the November output, where the model distinguishes terrain characteristics from the condensation process and assigns appropriate moisture values. For example, in this month, the original image failed to detect the elevated moisture levels associated with water body areas (August at Fig. 5). However, the downscaling process successfully identified the water body and correctly allocated high moisture values to that specific area. This highlights the strength of the downscaling technique in enhancing resolution and accuracy, particularly in detecting subtle moisture variations that might be overlooked in the original image.

5.2. Spatial and temporal accuracy assessment

5.2.1. Benefits of achieving 100 m resolution and its power to detect ground features

This higher level of soil moisture detail allows for optimizing resource use and ultimately improving crop yields. Such precision is not achievable with the coarser 1 Km downscaled data, which lacks the granularity needed to account for small-scale variations in soil moisture. Furthermore, the enhanced spatial resolution of 100 m data significantly benefits hydrological modeling. Accurate soil moisture inputs are crucial for predicting surface runoff, infiltration, and soil erosion. The finer spatial resolution of 100 m downscaled data improves the accuracy of these models, enabling better predictions and more effective management of water resources. In contrast, 1 Km downscaled data may overlook critical local variations, leading to less reliable hydrological assessments and predictions.

Moreover, the model's final outputs have demonstrated high accuracy in detecting soil moisture in challenging areas. Due to the influence of water bodies such as lakes on the brightness temperature received by SMAP satellite sensors (Du et al., 2016) and the utilization of the water fraction coefficient to determine the final moisture content, the moisture levels recorded over water bodies are generally among the lowest in the dataset (Ye et al., 2015). Therefore, identifying soil moisture in regions near these water bodies and accurately delineating their boundaries are crucial and challenging tasks. As illustrated in Fig. 11, which corresponds to May, the

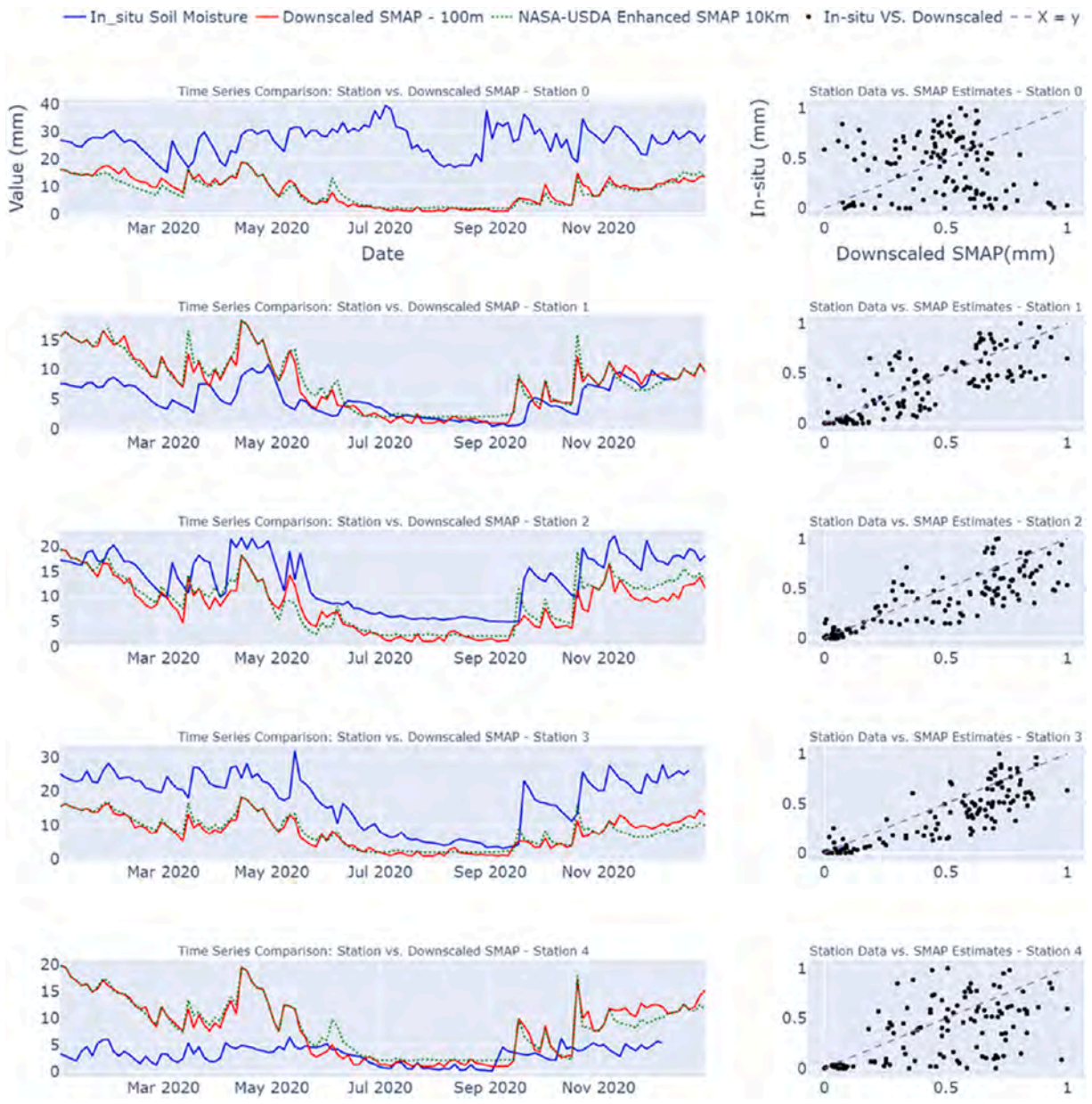

Fig. 7. Comparison of in-situ soil moisture with downscaled SMAP estimates: (Left) Time series; (Right) for the REMEDHUS stations.

downscaled images effectively detect the water body and the moisture in the surrounding lands. This precise allocation of water body values and adjacent soil moisture highlights the significant potential of these outputs for various applications requiring high-resolution soil moisture data. However, a notable limitation of our models is evident. As shown in Figs. 8 and 10, the availability of auxiliary data influences the model's performance. While the model effectively detects water bodies and estimates land moisture when sufficient cloud-free MODIS, Sentinel-2, and Landsat-9 images are accessible, its accuracy is lower during periods of extensive cloud cover. Future studies could investigate the impact of employing different masking techniques or focusing on coastal regions with expanded training datasets. By incorporating more diverse and region-specific data, researchers can potentially enhance model performance and improve the accuracy of water body detection and land moisture estimation. Cloud cover remains a significant challenge for optical-based downscaling approaches; however, in this study, the integration of microwave data and DEMs allowed the model to be trained effectively even under cloudy conditions. Additionally, leveraging both Sentinel-2 and Landsat-8 imagery, which have different revisit times, helped increase the availability of cloud-free observations for training, further supporting model robustness.

However, the amount of predicted data is not the same as the station record due to two main reasons. First, one important limitation in the validation of satellite-derived soil moisture against in-situ measurements lies in the inherent spatial scale mismatch between the two datasets. Ground stations provide point-based observations, whereas satellite products—particularly those derived from passive

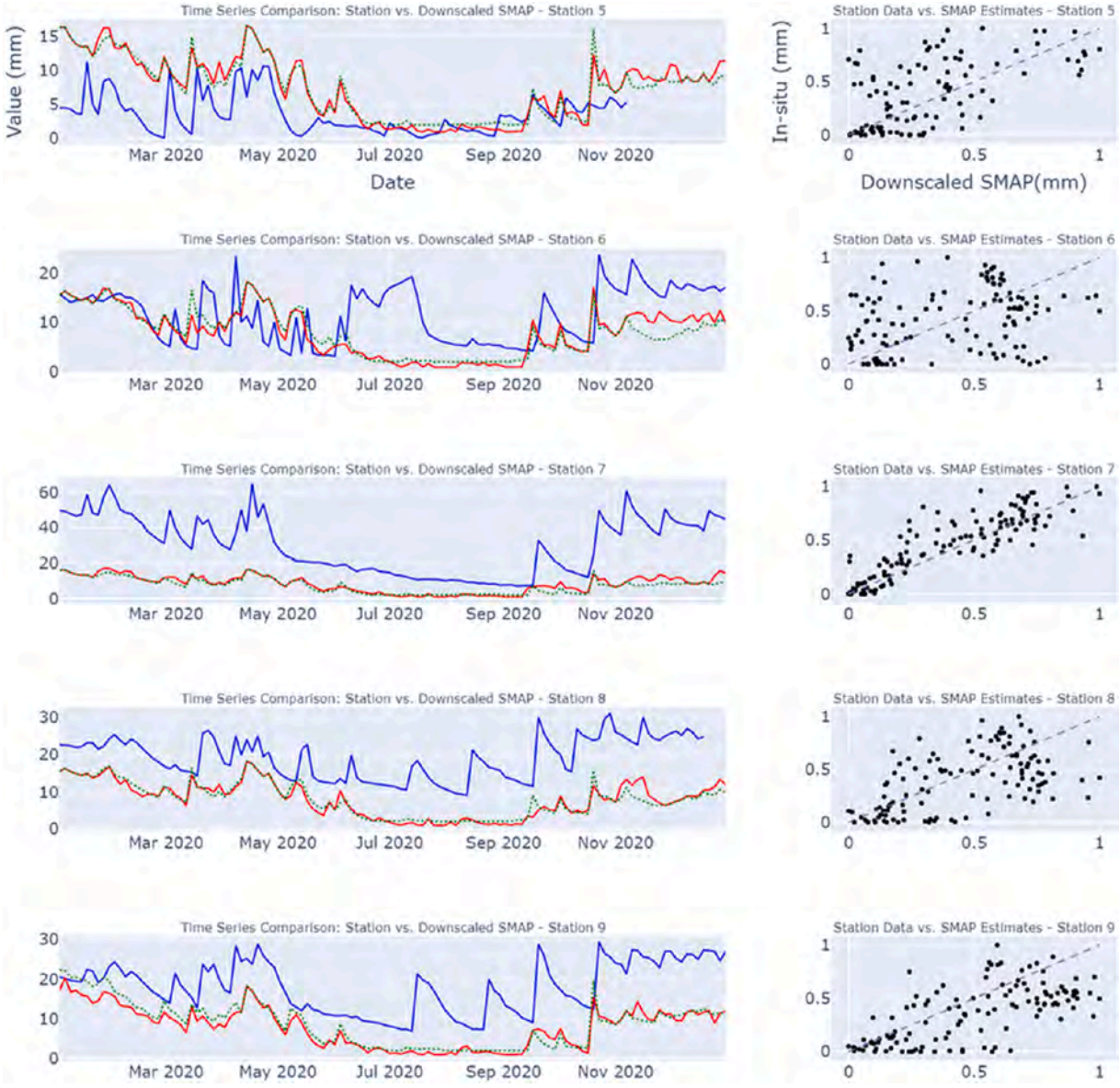

Fig. 8. Comparison of in-situ soil moisture with downscaled SMAP estimates: (Left) Time series; (Right) for the REMEDHUS stations (continued).

microwave sensors—represent soil moisture averaged over larger spatial footprints, often ranging from hundreds of meters to tens of kilometers. This discrepancy introduces uncertainty, as localized soil moisture variability within a satellite pixel—driven by factors such as vegetation, soil type, land cover, and topography—cannot be captured by a single point measurement. In this context, the temporal dynamics of point data may offer more relevant insights than direct comparison of absolute values, especially when high-resolution ground observations across the full satellite pixel are not available. Although our study does not implement spatial downscaling or representativeness filtering, we acknowledge this limitation and suggest that future work may benefit from incorporating such techniques (e.g., empirical, semi-empirical, or physically-based methods) to improve the robustness and accuracy of satellite validation efforts. Second, SMAP Enhanced product in GEE has a limitation of a maximum of 25 mm water in the top 5 cm of the soil layer which is fixed for agricultural use and it is not exactly what happens on bare soil and most common areas. For example, the SMAP time series at station 7 in Fig. 8 mimics the real-time series, but the moisture values are higher than half on most of the days, while our product does not increase as much as expected due to the limitation of the earth engine product. Furthermore, upon reviewing the soil composition at this station, it becomes evident that it primarily comprises clay soil (49 % clay and 51 % sand and silt), this type of soil exhibits a notable capacity for water retention, particularly in high-precipitation regions like there. At other stations, such as station 14 in Fig. 9, we observe significantly improved accuracy in terms of soil moisture values. Nonetheless, across all stations, the time series behavior is faithfully modeled, albeit with minor discrepancies in the absolute values. This consistency

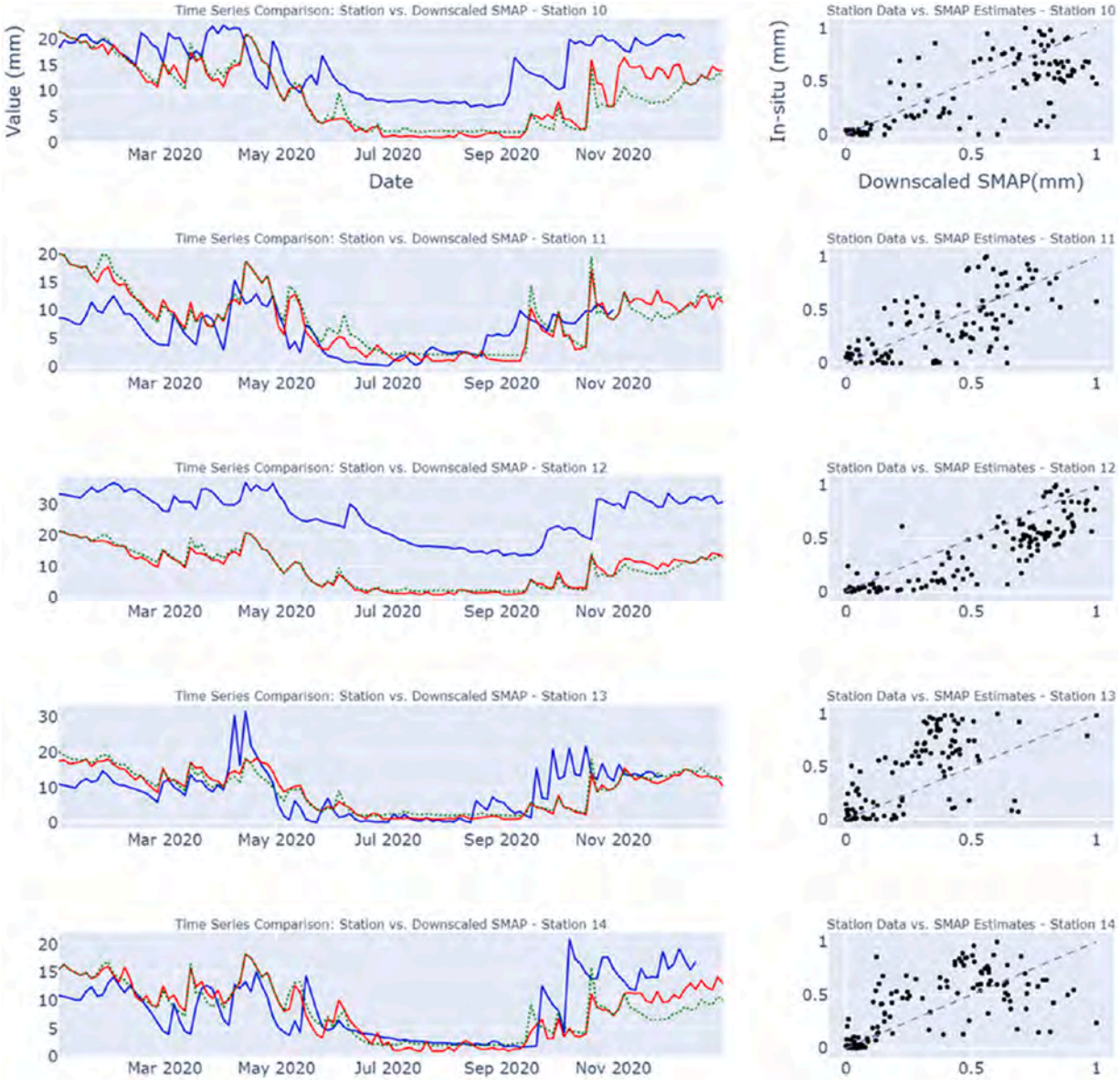

Fig. 9. Comparison of in-situ soil moisture with downscaled SMAP estimates: (Left) Time series; (Right) for the REMEDHUS stations (continued).

suggests that while the model may vary slightly in its quantification of soil moisture levels at different locations, it effectively captures the temporal dynamics of soil moisture fluctuations across the study area. Additionally, the error values for each station are presented in Fig. 12.

5.2.2. Time-series changes and SMAP pass times

The SMAP soil moisture downscaled product demonstrates its ability to capture anthropogenic influences, such as irrigation. Beyond this, it effectively responds to extreme rainfall events, as shown in Fig. 6, positioning it as a valuable tool for flood-related studies. The downscaled product accurately captured the soil moisture increase associated with intense rainfall events at station#99332 on November and station#40728 at the end of November. This capability highlights its potential for improving hydrological modeling and flood forecasting. In contrast, the original SMAP product maintained a relatively constant soil moisture trend during the late November and December rainfall events at station#40728. However, the extreme rainfall event in station#99292 on November 29, 2020, was not captured by either the downscaled or original SMAP product, likely due to the satellite's overpass time and soil moisture filtering processes. These findings underscore the importance of considering product limitations when analyzing extreme hydrological events.

Moreover, during the period from May to September, the coarse-resolution SMAP data remains relatively constant due to no

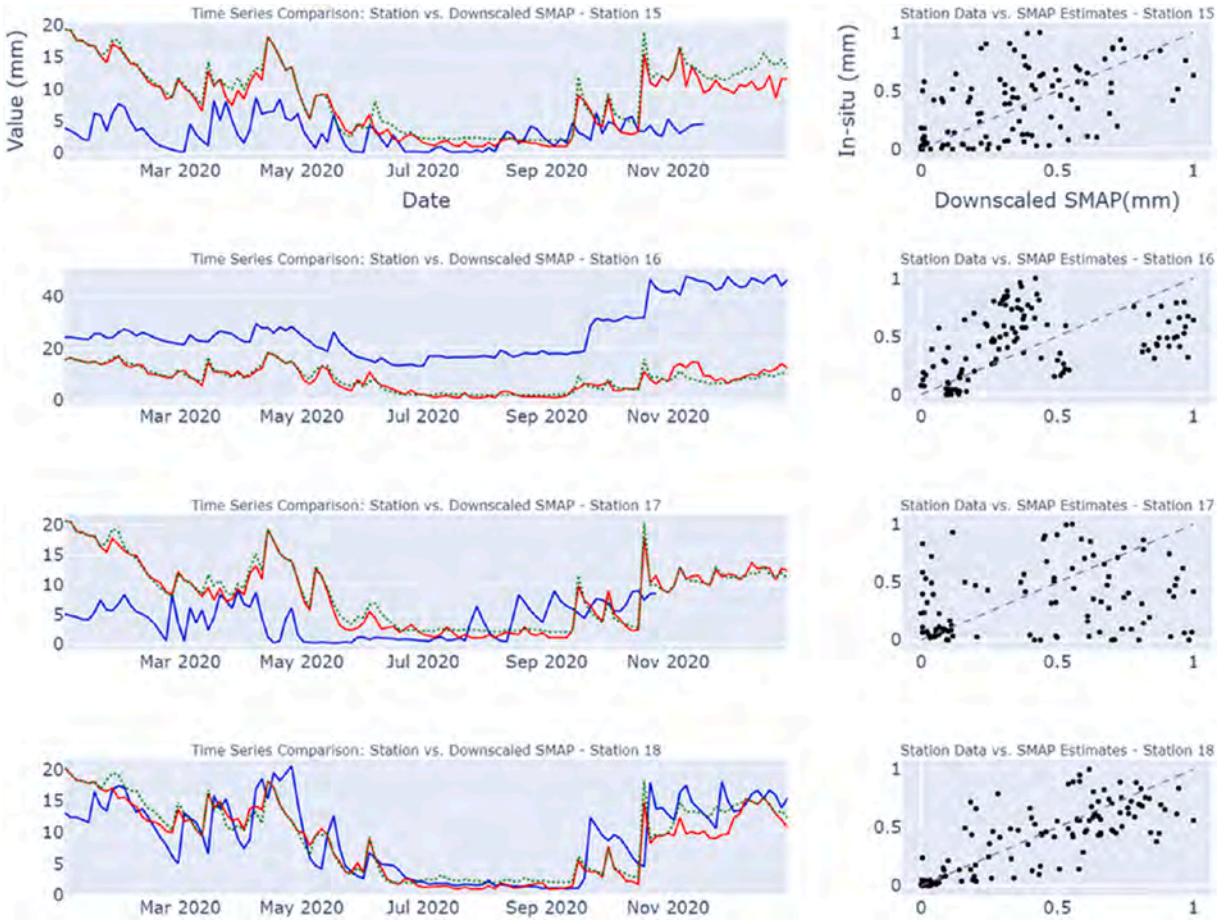

Fig. 10. Comparison of in-situ soil moisture with downscaled SMAP estimates: (Left) Time series; (Right) for the REMEDHUS stations (continued).

precipitation events. However, the downscaled soil moisture data exhibits noticeable fluctuations, which can be attributed to fine-scale processes such as irrigation and evaporation. the observed fluctuations in soil moisture (~5 mm in the top 50 cm layer) may seem relatively small compared to typical irrigation amounts. However, this can be attributed to the SMAP overpass time, which occurs around noon. By this time, a significant portion of the irrigation applied the previous day has either evaporated or infiltrated into deeper soil layers. As a result, the increase in soil moisture captured by SMAP appears moderate despite active irrigation.

It should mention that one important limitation in the validation of satellite-derived soil moisture against in-situ measurements lies in the inherent spatial scale mismatch between the two datasets. While ground stations provide point-based observations, satellite products—particularly those derived from passive microwave sensors—represent soil moisture averaged over large spatial footprints. This discrepancy introduces uncertainty, as localized soil moisture variability within a satellite pixel, influenced by heterogeneities in vegetation, soil type, land cover, and topography, is not captured by a single station. Consequently, direct one-to-one comparisons without addressing this mismatch may obscure meaningful interpretations. Although our study does not employ spatial downscaling methods, we acknowledge this limitation and emphasize that future work may benefit from incorporating downscaling techniques (e.g., empirical, semi-empirical, or physically-based methods) or applying spatial representativeness filters to improve the robustness of validation.

6. Conclusion

This study presents a novel approach to downscaling SMAP soil moisture using a random forest model tailored to each target SMAP image. By strategically selecting training data and applying a unique model for each image, we significantly reduced computational costs compared to previous studies while maintaining comparable accuracy.

Our results demonstrate the effectiveness of the proposed method in capturing spatial heterogeneity and temporal dynamics of soil moisture. The downscaled product exhibits strong correlations with precipitation and accurately represents various land cover features, including water bodies and different crop types. Successful applications in both arid/semi-arid and humid regions highlight the versatility of the model.

This research contributes to the field by introducing a new paradigm for downscaling soil moisture and showcasing the potential of

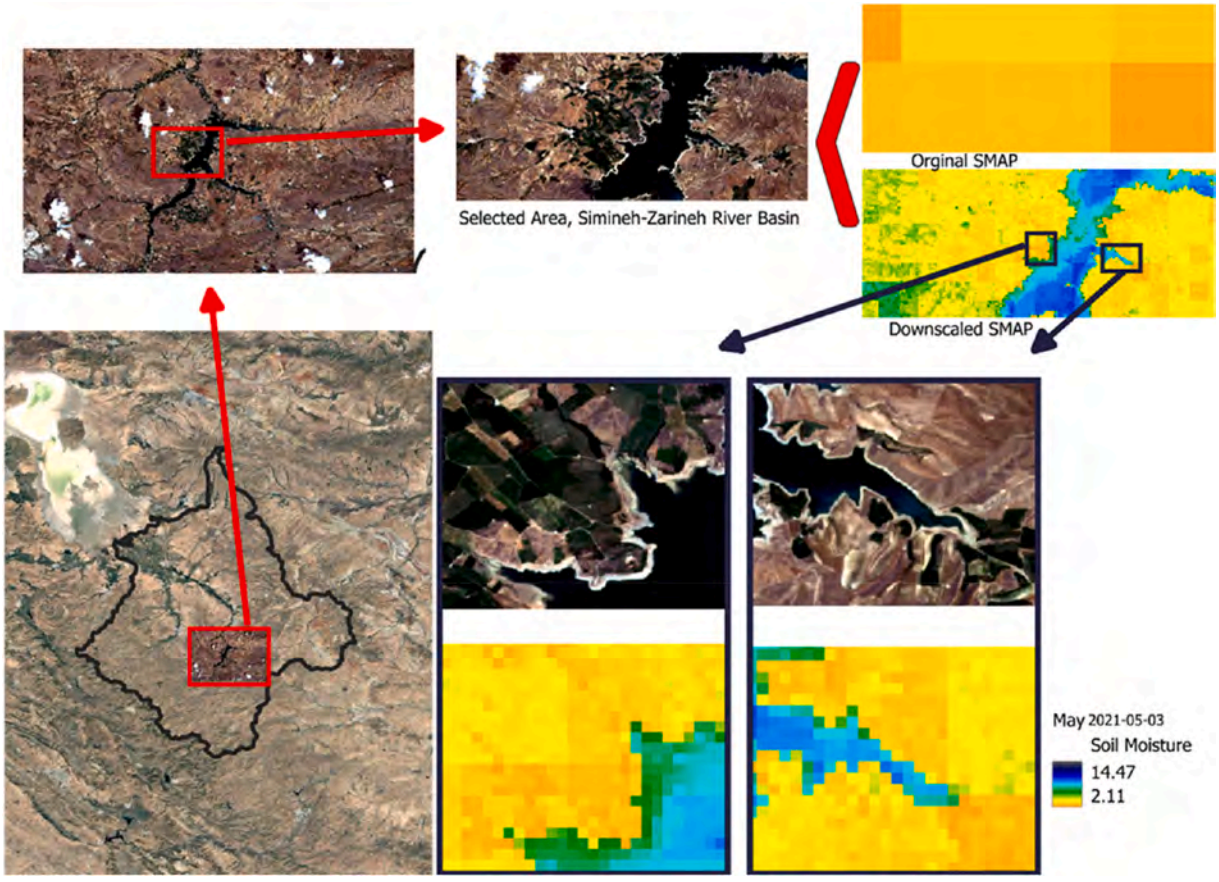

Fig. 11. Detailed soil moisture map for a selected area near the water body.

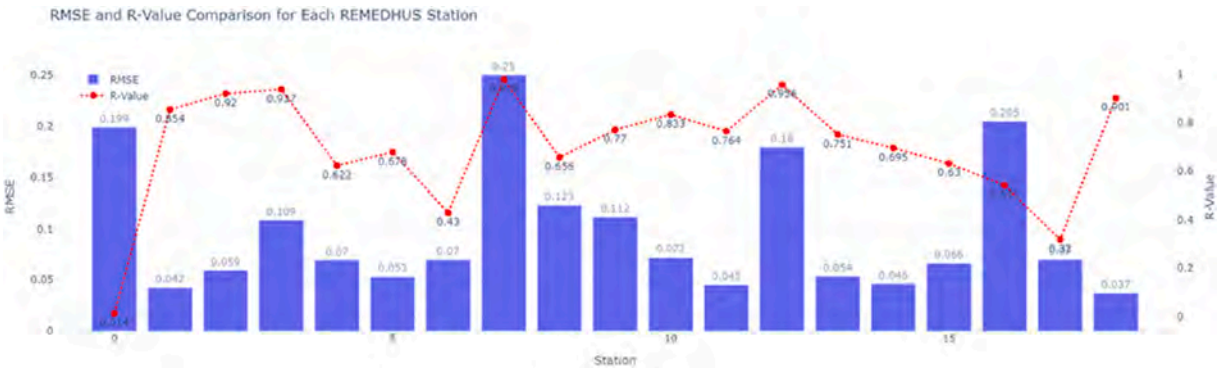

Fig. 12. Comparison of RMSE (blue bars) and R-value (red markers) for soil moisture estimation at REMEDHUS stations.

cloud computing to accelerate the modeling process. The generation of high-resolution soil moisture data (100 m) opens up new opportunities for precision agriculture and improved hydrological modeling.

While this study focuses on Random Forest due to its proven performance, computational efficiency, and native support in Google Earth Engine, we acknowledge the value of comparing multiple machine learning models. Future research could explore benchmark comparisons with other tree-based or ensemble methods (e.g., XGBoost) and deep learning approaches where feasible, especially in local or smaller-scale studies where platform constraints are less prohibitive. This would further refine the selection of optimal models for different environmental and computational contexts.

CRediT authorship contribution statement

Mohsen Moghaddas: Writing – review & editing, Writing – original draft, Visualization, Validation, Software, Methodology, Formal analysis, Data curation, Conceptualization. **Massoud Tajrishy:** Supervision, Conceptualization.

Code availability

The computer algorithms created in this research can be obtained from the corresponding author upon a reasonable request.

Ethical statement

This research was conducted in adherence to the ethical guidelines of *Remote Sensing Applications: Society and Environment* and institutional standards. The study exclusively used open-source and publicly available datasets, specifically from the International Soil Moisture Network (ISMN), along with remote sensing data and precipitation data obtained from the Iranian Meteorological Organization. No new data were collected, and no human or animal subjects were involved.

As a result, institutional ethics approval was deemed unnecessary. All data sources are properly cited, and data use complies with the respective licensing agreements, ensuring full transparency and ethical responsibility.

Any potential conflicts of interest have been addressed separately in the Declaration of Interest Statement.

Declaration of competing interest

The authors declare that they have no known competing financial interests or personal relationships that could have appeared to influence the work reported in this paper.

Data availability

Data will be made available on request.

References

Abushandi, E., 2016. Flash flood simulation for Tabuk city catchment, Saudi Arabia. Arabian J. Geosci. 9 (3), 188. https://doi.org/10.1007/s12517-015-2192-x.

Amazirh, A., Merlin, O., Er-Raki, S., 2019. Including Sentinel-1 radar data to improve the disaggregation of MODIS land surface temperature data. ISPRS J. Photogrammetry Remote Sens. 150, 11–26. https://doi.org/10.1016/j.isprsjprs.2019.02.004.

Bai, J., Cui, Q., Zhang, W., Meng, L., 2019. An approach for downscaling SMAP soil moisture by combining Sentinel-1 SAR and MODIS data. Remote Sens. 11 (23), 2736. https://doi.org/10.3390/rs11232736.

Breiman, L., 2001. [no title found]. Mach. Learn. 45 (1), 5–32. https://doi.org/10.1023/A:1010933404324.

Brocca, L., Melone, F., Moramarco, T., Morbidelli, R., 2010. Spatial-temporal variability of soil moisture and its estimation across scales: soil MOISTURE SPATIOTEMPORAL VARIABILITY. Water Resour. Res. 46 (2). https://doi.org/10.1029/2009WR008016.

Brocca, L., Tullo, T., Melone, F., Moramarco, T., Morbidelli, R., 2012. Catchment scale soil moisture spatial–temporal variability. J. Hydrol. 422–423, 63–75. https://doi.org/10.1016/j.jhydrol.2011.12.039.

Brocca, L., Zhao, W., Lu, H., 2023. High-resolution observations from space to address new applications in hydrology. Innovation 4 (3), 100437. https://doi.org/10.1016/j.xinn.2023.100437.

Ceballos, A., Scipal, K., Wagner, W., Martínez-Fernández, J., 2005. Validation of ERS scatterometer-derived soil moisture data in the central part of the Duero Basin, Spain. Hydrol. Process. 19 (8), 1549–1566. https://doi.org/10.1002/hyp.5585.

Chander, G., Markham, B.L., Helder, D.L., 2009. Summary of current radiometric calibration coefficients for Landsat MSS, TM, ETM+, and EO-1 ALI sensors. Remote Sens. Environ. 113 (5), 893–903. https://doi.org/10.1016/j.rse.2009.01.007.

Chauhan, N.S., Miller, S., Ardanuy, P., 2003. Spaceborne soil moisture estimation at high resolution: a microwave-optical/IR synergistic approach. Int. J. Rem. Sens. 24 (22), 4599–4622. https://doi.org/10.1080/0143116031000156837.

Chen, Q., Miao, F., Wang, H., Xu, Z., Tang, Z., Yang, L., Qi, S., 2020. Downscaling of satellite remote sensing soil moisture products over the Tibetan Plateau based on the random Forest algorithm: preliminary results. Earth Space Sci. 7 (6), e2020EA001265. https://doi.org/10.1029/2020EA001265.

Chen, Q., Zeng, J., Cui, C., Li, Z., Chen, K.-S., Bai, X., Xu, J., 2018. Soil moisture retrieval from SMAP: a validation and error analysis Study using ground-based observations over the little washita watershed. IEEE Trans. Geosci. Rem. Sens. 56 (3), 1394–1408. https://doi.org/10.1109/TGRS.2017.2762462.

Chi, M., Plaza, A., Benediktsson, J.A., Sun, Z., Shen, J., Zhu, Y., 2016. Big data for remote sensing: challenges and opportunities. Proc. IEEE 104 (11), 2207–2219. https://doi.org/10.1109/JPROC.2016.2598228.

Choi, M., Hur, Y., 2012. A microwave-optical/infrared disaggregation for improving spatial representation of soil moisture using AMSR-E and MODIS products. Remote Sens. Environ. 124, 259–269. https://doi.org/10.1016/j.rse.2012.05.009.

Cochran, W.G., 1946. Relative accuracy of systematic and stratified random samples for a certain class of populations. Ann. Math. Stat. 17 (2), 164–177. https://doi.org/10.1214/aoms/1177730978.

De Queiroz, M.G., Da Silva, T.G.F., Zolnier, S., Jardim, A.M.D.R.F., De Souza, C.A.A., Araújo Júnior, G.D.N., De Morais, J.E.F., De Souza, L.S.B., 2020. Spatial and temporal dynamics of soil moisture for surfaces with a change in land use in the semi-arid region of Brazil. Catena 188, 104457. https://doi.org/10.1016/j.catena.2020.104457.

Djamali, M., de Beaulieu, J.-L., Shah-hosseini, M., Andrieu-Ponel, V., Ponel, P., Amini, A., Akhani, H., Leroy, S.A.G., Stevens, L., Lahijani, H., Brewer, S., 2008. A late Pleistocene long pollen record from Lake Urmia, Nw Iran. Quat. Res. 69 (3), 413–420. https://doi.org/10.1016/j.yqres.2008.03.004.

Du, J., Kimball, J.S., Jones, L.A., Watts, J.D., 2016. Implementation of satellite based fractional water cover indices in the pan-Arctic region using AMSR-E and MODIS. Remote Sens. Environ. 184, 469–481. https://doi.org/10.1016/j.rse.2016.07.029.

El Hajj, M., Baghdadi, N., Zribi, M., Bazzi, H., 2017. Synergic use of Sentinel-1 and Sentinel-2 images for operational soil moisture mapping at high spatial resolution over agricultural areas. Remote Sens. 9 (12), 1292. https://doi.org/10.3390/rs9121292.

Entekhabi, D., Njoku, E.G., O'Neill, P.E., Kellogg, K.H., Crow, W.T., Edelstein, W.N., Entin, J.K., Goodman, S.D., Jackson, T.J., Johnson, J., Kimball, J., Piepmeier, J. R., Koster, R.D., Martin, N., McDonald, K.C., Moghaddam, M., Moran, S., Reichle, R., Shi, J.C., et al., 2010. The Soil Moisture Active Passive (SMAP) Mission. Proc. IEEE 98 (5), 704–716. https://doi.org/10.1109/JPROC.2010.2043918.

Fletcher, K., Agency, European Space (Eds.), 2012. Sentinel-1: Esa's Radar Observatory Mission for GMES Operational Services. ESA Communications.
Gao, M., Zhu, K., Guo, Y., Han, X., Li, D., Zhang, S., 2024. Downscaling SMAP soil moisture product in cold and arid region: incorporating NDSI and BSI into the random forest algorithm. Vadose Zone J. 23 (3), e20323. https://doi.org/10.1002/vzj2.20323.
Gascon, F., Bouzinac, C., Thépaut, O., Jung, M., Francesconi, B., Louis, J., Lonjou, V., Lafrance, B., Massera, S., Gaudel-Vacaresse, A., Languille, F., Alhammoud, B., Viallefont, F., Pflug, B., Bieniarz, J., Clerc, S., Pessiot, L., Trémas, T., Cadau, E., et al., 2017. Copernicus Sentinel-2A calibration and products validation status. Remote Sens. 9 (6), 584. https://doi.org/10.3390/rs9060584.
Han, J., Mao, K., Xu, T., Guo, J., Zuo, Z., Gao, C., 2018. A soil moisture estimation framework based on the CART algorithm and its application in China. J. Hydrol. 563, 65–75. https://doi.org/10.1016/j.jhydrol.2018.05.051.
He, L., Hong, Y., Wu, X., Ye, N., Walker, J.P., Chen, X., 2018. Investigation of SMAP active–passive downscaling algorithms using combined Sentinel-1 SAR and SMAP radiometer data. IEEE Trans. Geosci. Rem. Sens. 56 (8), 4906–4918. https://doi.org/10.1109/TGRS.2018.2842153.
Im, J., Park, S., Rhee, J., Baik, J., Choi, M., 2016. Downscaling of AMSR-E soil moisture with MODIS products using machine learning approaches. Environ. Earth Sci. 75 (15), 1120. https://doi.org/10.1007/s12665-016-5917-6.
Jin, Y., Ge, Y., Liu, Y., Chen, Y., Zhang, H., Heuvelink, G.B.M., 2021. A machine learning-based geostatistical downscaling method for coarse-resolution soil moisture products. IEEE J. Sel. Top. Appl. Earth Obs. Rem. Sens. 14, 1025–1037. https://doi.org/10.1109/JSTARS.2020.3035386.
Kerr, Y.H., Waldteufel, P., Wigneron, J.-P., Delwart, S., Cabot, F., Boutin, J., Escorihuela, M.-J., Font, J., Reul, N., Gruhier, C., Juglea, S.E., Drinkwater, M.R., Hahne, A., Martín-Neira, M., Mecklenburg, S., 2010. The SMOS Mission: new tool for monitoring key elements ofthe global water cycle. Proc. IEEE 98 (5), 666–687. https://doi.org/10.1109/JPROC.2010.2043032.
Kim, S., Paik, K., Johnson, F.M., Sharma, A., 2018. Building a flood-warning framework for ungauged locations using low resolution, open-access remotely sensed surface soil moisture, precipitation, soil, and topographic information. IEEE J. Sel. Top. Appl. Earth Obs. Rem. Sens. 11 (2), 375–387. https://doi.org/10.1109/JSTARS.2018.2790409.
Koster, R.D., Crow, W.T., Reichle, R.H., Mahanama, S.P., 2018. Estimating basin-scale water budgets with SMAP soil moisture data. Water Resour. Res. 54 (7), 4228–4244. https://doi.org/10.1029/2018WR022669.
Ma, H., Zeng, J., Chen, N., Zhang, X., Cosh, M.H., Wang, W., 2019. Satellite surface soil moisture from SMAP, SMOS, AMSR2 and ESA CCI: a comprehensive assessment using global ground-based observations. Remote Sens. Environ. 231, 111215. https://doi.org/10.1016/j.rse.2019.111215.
Mao, T., Shangguan, W., Li, Q., Li, L., Zhang, Y., Huang, F., Li, J., Liu, W., Zhang, R., 2022. A spatial downscaling method for remote sensing soil moisture based on random Forest considering soil moisture memory and mass conservation. Remote Sens. 14 (16), 3858. https://doi.org/10.3390/rs14163858.
Martens, B., Miralles, D., Lievens, H., Fernández-Prieto, D., Verhoest, N.E.C., 2016. Improving terrestrial evaporation estimates over continental Australia through assimilation of SMOS soil moisture. Int. J. Appl. Earth Obs. Geoinf. 48, 146–162. https://doi.org/10.1016/j.jag.2015.09.012.
Martínez-Fernández, J., González-Zamora, A., Almendra-Martín, L., 2021. Soil moisture memory and soil properties: an analysis with the stored precipitation fraction. J. Hydrol. 593, 125622. https://doi.org/10.1016/j.jhydrol.2020.125622.
Martínez-Fernández, J., González-Zamora, A., Sánchez, N., Gumuzzio, A., Herrero-Jiménez, C.M., 2016. Satellite soil moisture for agricultural drought monitoring: assessment of the SMOS derived soil Water Deficit Index. Remote Sens. Environ. 177, 277–286. https://doi.org/10.1016/j.rse.2016.02.064.
McColl, K.A., He, Q., Lu, H., Entekhabi, D., 2019. Short-Term and long-term surface soil moisture memory time scales are spatially anticorrelated at global scales. J. Hydrometeorol. 20 (6), 1165–1182. https://doi.org/10.1175/JHM-D-18-0141.1.
Ochsner, T.E., Cosh, M.H., Cuenca, R.H., Dorigo, W.A., Draper, C.S., Hagimoto, Y., Kerr, Y.H., Larson, K.M., Njoku, E.G., Small, E.E., Zreda, M., 2013. State of the art in large-scale soil moisture monitoring. Soil Sci. Soc. Am. J. 77 (6), 1888–1919. https://doi.org/10.2136/sssaj2013.03.0093.
Owe, M., Van de Griend, A.A., 1998. Comparison of soil moisture penetration depths for several bare soils at two microwave frequencies and implications for remote sensing. Water Resour. Res. 34 (9), 2319–2327. https://doi.org/10.1029/98WR01469.
Pablos, M., Piles, M., Sánchez, N., Vall-llossera, M., Martínez-Fernández, J., Camps, A., 2016. Impact of day/night time land surface temperature in soil moisture disaggregation algorithms. European Journal of Remote Sensing 49 (1), 899–916. https://doi.org/10.5721/EuJRS20164947.
Peng, J., Loew, A., Merlin, O., Verhoest, N.E.C., 2017. A review of spatial downscaling of satellite remotely sensed soil moisture: Downscale Satellite-Based Soil Moisture. Rev. Geophys. 55 (2), 341–366. https://doi.org/10.1002/2016RG000543.
Peng, J., Niesel, J., Loew, A., 2015. Evaluation of soil moisture downscaling using a simple thermal-based proxy – the REMEDHUS network (Spain) example. Hydrol. Earth Syst. Sci. 19 (12), 4765–4782. https://doi.org/10.5194/hess-19-4765-2015.
Petropoulos, G.P., Ireland, G., Barrett, B., 2015. Surface soil moisture retrievals from remote sensing: current status, products & future trends. Phys. Chem. Earth, Parts A/B/C 83–84, 36–56. https://doi.org/10.1016/j.pce.2015.02.009.
Piles, M., Camps, A., Vall-llossera, M., Corbella, I., Panciera, R., Rudiger, C., Kerr, Y.H., Walker, J., 2011. Downscaling SMOS-Derived soil moisture using MODIS visible/Infrared data. IEEE Trans. Geosci. Rem. Sens. 49 (9), 3156–3166. https://doi.org/10.1109/TGRS.2011.2120615.
Piles, M., Sanchez, N., Vall-llossera, M., Camps, A., Martinez-Fernandez, J., Martinez, J., Gonzalez-Gambau, V., 2014. A downscaling approach for SMOS land observations: evaluation of high-resolution soil moisture maps over the iberian peninsula. IEEE J. Sel. Top. Appl. Earth Obs. Rem. Sens. 7 (9), 3845–3857. https://doi.org/10.1109/JSTARS.2014.2325398.
Purdy, A.J., Fisher, J.B., Goulden, M.L., Colliander, A., Halverson, G., Tu, K., Famiglietti, J.S., 2018. SMAP soil moisture improves global evapotranspiration. Remote Sens. Environ. 219, 1–14. https://doi.org/10.1016/j.rse.2018.09.023.
Sabaghy, S., Walker, J.P., Renzullo, L.J., Jackson, T.J., 2018. Spatially enhanced passive microwave derived soil moisture: capabilities and opportunities. Remote Sens. Environ. 209, 551–580. https://doi.org/10.1016/j.rse.2018.02.065.
Sánchez, N., González-Zamora, Á., Martínez-Fernández, J., Piles, M., Pablos, M., 2018. Integrated remote sensing approach to global agricultural drought monitoring. Agric. For. Meteorol. 259, 141–153. https://doi.org/10.1016/j.agrformet.2018.04.022.
Sánchez-Ruiz, S., Piles, M., Sánchez, N., Martínez-Fernández, J., Vall-llossera, M., Camps, A., 2014. Combining SMOS with visible and near/shortwave/thermal infrared satellite data for high resolution soil moisture estimates. J. Hydrol. 516, 273–283. https://doi.org/10.1016/j.jhydrol.2013.12.047.
Santi, E., Paloscia, S., Pettinato, S., Brocca, L., Ciabatta, L., Entekhabi, D., 2018. On the synergy of SMAP, AMSR2 AND SENTINEL-1 for retrieving soil moisture. Int. J. Appl. Earth Obs. Geoinf. 65, 114–123. https://doi.org/10.1016/j.jag.2017.10.010.
Sishah, S., Abrahem, T., Azene, G., Dessalew, A., Hundera, H., 2023. Downscaling and validating SMAP soil moisture using a machine learning algorithm over the Awash River basin, Ethiopia. PLoS One 18 (1), e0279895. https://doi.org/10.1371/journal.pone.0279895.
Ye, N., Walker, J.P., Guerschman, J., Ryu, D., Gurney, R.J., 2015. Standing water effect on soil moisture retrieval from L-band passive microwave observations. Remote Sens. Environ. 169, 232–242. https://doi.org/10.1016/j.rse.2015.08.013.
Zhao, W., Li, A., 2013. A downscaling method for improving the spatial resolution of AMSR-E derived soil moisture product based on MSG-SEVIRI data. Remote Sens. 5 (12), 6790–6811. https://doi.org/10.3390/rs5126790.
Zhao, W., Sánchez, N., Lu, H., Li, A., 2018. A spatial downscaling approach for the SMAP passive surface soil moisture product using random forest regression. J. Hydrol. 563, 1009–1024. https://doi.org/10.1016/j.jhydrol.2018.06.081.